Chemistry–A European Journal
Research Article
doi.org/10.1002/chem.202300214
Chemistry Europe
European Chemical Societies Publishing
www.chemeurj.org

C–H Functionalization of Heterocycles with Triplet Carbenes by means of an Unexpected 1,2-Alkyl Radical Migration**

Claire Empel,[a] Sripati Jana,[a] Łukasz W. Ciszewski,[b] Katarzyna Zawada,[c] Chao Pei,[a] Dorota Gryko,*[b] and Rene M. Koenigs*[a]

Abstract: The C–H functionalization of indole heterocycles constitutes a key strategy to leverage the synthesis of endogenous signaling molecules such as tryptamine or tryptophol. Herein, we report on the photocatalytic reaction of ethyl diazoacetate with indole, which shows an unusual solvent dependency. While C2-functionalization occurs under protic conditions, the use of aprotic solvents leads to a complete reversal of selectivity and exclusive C3-functionalization occurs. To rationalize for this unexpected reactivity switch, we have conducted detailed theoretical and experimental studies, which suggest the participation of a triplet carbene intermediate that undergoes initial C2-functionalization. A distinct cationic [1,2]-alkyl radical migration then leads to formation of C3-functionalized indole. We conclude with the application of this photocatalytic reaction to access oxidized tryptophol derivatives including gram-scale synthesis and derivatization reactions.

Introduction

Tryptophol was first described in 1912 by Ehrlich via enzymatic degradation of tryptophan with yeast and induces sleep in humans.[1,2] Its derivatives can be isolated from a plethora of natural sources, such as bacteria, fungi, and plants and the tryptophol motif is an essential molecular scaffold in many natural products (Scheme 1a).[3,4] From an organic synthetic perspective, tryptophol and its derivatives can be readily obtained in a biomimetic fashion via deamination and reduction of the amino acid tryptophan,[5] or in an alkylation reaction of indole.[6–16] To achieve such alkylations, the reaction of indole heterocycles with diazoalkanes recently emerged as an important strategy that allows the catalytic or photochemical introduction of a carbene fragment into the C-3 position of protected and unprotected indole heterocycles.[7–13] Notable advances in this research area include the development of enantioselective C–H functionalization reactions with donor/acceptor diazoalkanes,[9,10] applications in tryptamine synthesis with diazoacetonitrile,[7] biocatalytic C–H functionalization reactions,[7,11,12] or the synthesis of *gem*-difluoro olefins using fluorinated diazo compounds.[13]

Despite these advances, current literature surprisingly lacks rigorous investigations on the reaction mechanism and pathways involving direct C–H functionalization in the C3 position[7–10] or a cyclopropanation-ring opening reaction mechanism are under discussion. The latter has been described in the copper-catalyzed reaction of ethyl diazoacetate via singlet carbene intermediates.[8] On the contrary, current data on the mechanism of iron-catalyzed C3-functionalization with diazoacetonitrile suggests the participation of intermediates with unpaired electrons,[7] which seems counterintuitive and should result - similar to radical processes - in C2-functionalization of indole. Such radical process was recently described using ethyl diazoacetate under photocatalytic conditions (Scheme 1b).[16] As such, the mechanism of indole functionalization remains an ongoing riddle and more sophisticated investigations are in high demand for a thorough understanding of underlying reaction pathways.

Herein, we report on a combined experimental and theoretical study on the photocatalytic reaction of indole with alkyl diazoacetates (Scheme 1c). We discuss pathways of the photocatalytic decomposition of alkyl diazoacetates to rationalize the formation of reactive intermediate species. This process involves the reaction of a triplet carbene intermediate,

[a] C. Empel, S. Jana, C. Pei, Prof. Dr. R. M. Koenigs
RWTH Aachen University
Institute of Organic Chemistry
Landoltweg 1, 52074 Aachen (Germany)
E-mail: rene.koenigs@rwth-aachen.de
[b] Ł. W. Ciszewski, Prof. Dr. D. Gryko
Polish Academy of Sciences
Institute of Organic Chemistry
Kasprzaka 44/52, 01–224 Warsaw (Poland)
E-mail: dorota.gryko@icho.edu.pl
[c] Dr. K. Zawada
Medical University of Warsaw
Faculty of Pharmacy
Banacha 1, 02-097 Warsaw (Poland)

[**] A previous version of this manuscript has been deposited on a preprint server (https://doi.org/10.26434/chemrxiv-2022-2pmzq).

Supporting information for this article is available on the WWW under https://doi.org/10.1002/chem.202300214

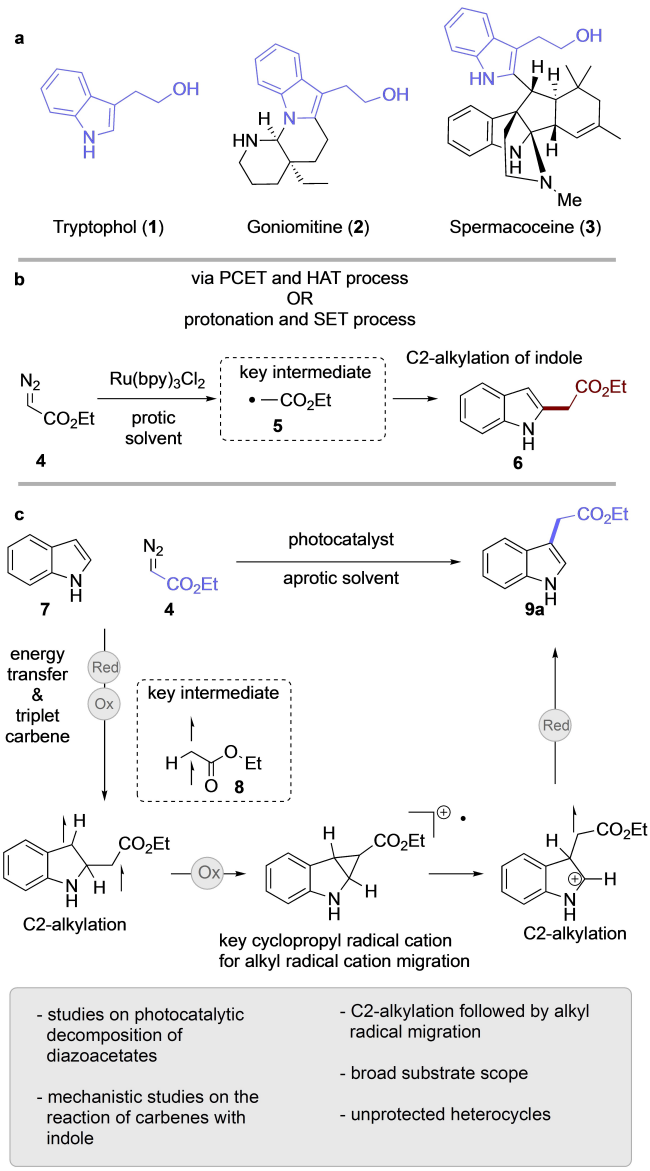

Scheme 1. a. Naturally occurring analogues of tryptophol. b. Photocatalytic C2-functionalization of indole in protic solvent. c. C3-functionalization via alkyl radical migration.

which undergoes initial C2-functionalization. Photocatalysis then unlocks pathways towards a formal 1,2-alkyl radical cation migration leading to the formation of the thermodynamically favored C3-alkylation product.

Results and Discussion

With the goal of understanding the fundamentals of indole C–H functionalization and the development of synthetic methods for tryptophol synthesis, we commenced our investigations by studying the reaction of ethyl diazoacetate with indole under photochemical conditions via free carbene intermediates. To overcome limitations of weak absorbance of ethyl diazoacetate (EDA) in the visible light region, we employed photosensitizers as a handle to facilitate its photolysis,[16,19–24] and to promote the formation of carbene intermediates via an energy transfer process.[21,22] In initial studies, we therefore examined the role of the reaction medium and observed a surprising solvent dependency of indole C–H functionalization. In accordance to previous work by Gryko and co-workers,[16] a good chemoselectivity for C2 functionalization was observed in protic solvents. However, a complete unexpected reversal of selectivity was observed in DCM solvent and C3 functionalization occurred in excellent regioselectivity (>20:1). No by-product from competing N–H functionalization was detected under both reaction conditions. This outcome suggests a significant influence of protic solvents on the reaction outcome and we therefore examined the influence of methanol on the reaction in DCM and observed a significant solvent dependency of product distribution (Scheme 2). While the addition of 10 equivalents of methanol resulted in a 1:1 distribution of C2- and C3-alkylation products, an almost complete switch to C2-alkylation was observed when adding more then 60 equivalents of methanol.

Studies on the photocatalytic decomposition of ethyl diazoacetate

This surprising selective solvent-dependent reaction outcome prompted us next at rationalizing the divergent reactivity of EDA under dye-sensitized conditions. We performed a Stern Volmer experiment of the photocatalyst and both reactants (Scheme 3a). In both DCM and MeOH solvents, we observed fluorescence quenching near the diffusion limit in the presence of ethyl diazoacetate (DCM: $k_q = 8.6 \times 10^8\ M^{-1}s^{-1}$, MeOH: $k_q = 4.3 \times 10^8\ M^{-1}s^{-1}$), while a weaker fluorescence quenching was observed in the presence of indole (Scheme 3a). This observa-

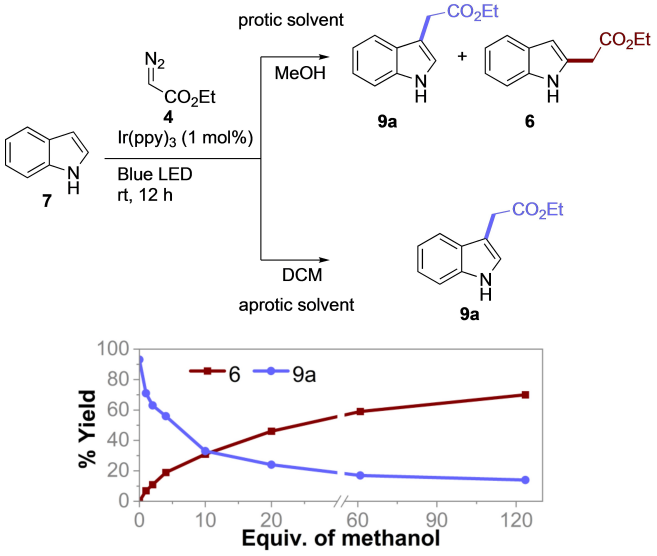

Scheme 2. Investigations on the influence of solvent on the C–H functionalization of unprotected indole.

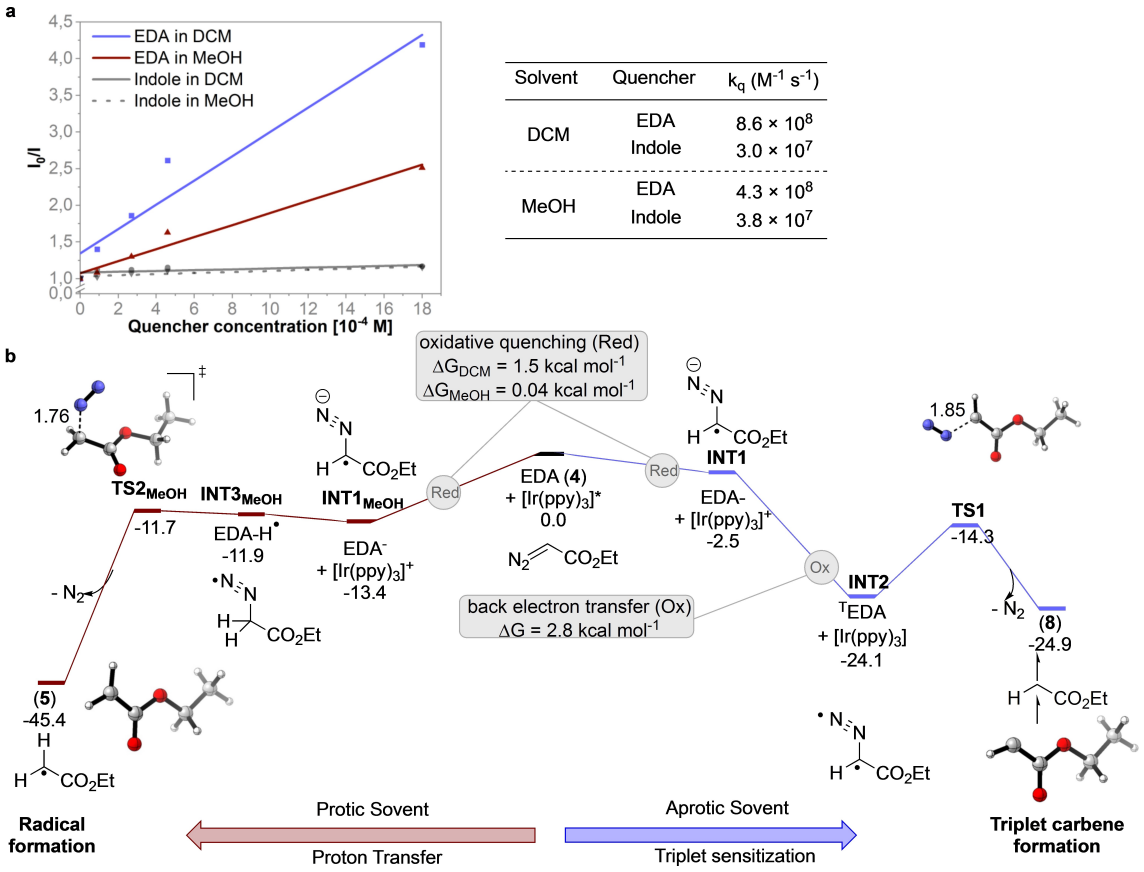

Scheme 3. Investigations on the influence of solvent on the photocatalytic decomposition of EDA. a. Stern-Volmer experiment. b. Mechanism of the photocatalytic decomposition of EDA. Calculations were performed at the (U)M06-2X-D3/def2-TZVPP // (U)B3LYP–D3BJ/def2-SVP/def2-TZVPP level of theory using SMD (DCM) solvent model.

tion suggests that ethyl diazoacetate and the iridium photocatalyst may interact by both electron or energy transfer in DCM and MeOH solvents.

To further deconvolute energy and electron transfer, we examined this key step by DFT calculations and probed the viability of electron, energy, and proton transfer pathways (Scheme 3b). First, the oxidative quenching of $Ir(ppy)_3$* with ethyl diazoacetate, which is a thermodynamically feasible reduction in MeOH solvent, was evaluated. In DCM solvent, however, such reduction is less favored and results in a process that involves a double electron transfer to give the triplet state of EDA (for the analysis of triplet energies, please see Figure S1). The latter undergoes a facile extrusion of nitrogen gas to give a triplet carbene.

Finally, we analyzed proton transfer pathways and examined an equilibrium between ethyl diazoacetate, methanol, and the corresponding diazonium ion. Calculations show that such protonation of ethyl diazoacetate with MeOH is not feasible ($\Delta G^{\ddagger} = 34.0$ kcal mol^{-1}, for details, please see Figure S2), instead protonation of the reduced form of EDA can occur without an energy barrier to give a diazonium ion intermediate INT3 (Scheme 3b left), that finally leads to the formation of an alkyl radical and nitrogen extrusion. Thus, depending on the solvent either energy or electron transfer processes are at play that in turn lead to formation of triplet carbene or radical intermediates, respectively.

C3-alkylation reaction

Based on the large singlet/triplet energy splitting, we turned our attention to the reaction of the triplet carbene intermediate (Scheme 4a,b). As expected, the triplet carbene undergoes addition to the C2 position of indole (**TS3**), which is energetically preferred by 1.9 kcal mol^{-1} over C3 addition (**TS4**). Based on the observed reaction outcome this initial C2-functionalization seems counterintuitive, however, calculations show that **INT4** can undergo an unusual 1,2-migration reaction of an alkyl radical. This reaction sequence is initiated by one-electron oxidation of **INT4** to give radical cation **INT5**. This oxidation step can occur from either the photoexcited state $[Ir(III)ppy_3]$* or from the oxidized species $[Ir(IV)ppy_3]^+$ and can thus occur via both reductive or oxidative quenching pathways (for details, see Figure S4). This radical cation **INT5** undergoes a facile 1,2-alkyl radical migration via cyclopropane radical cation **INT6** and ring opening to give the thermodynamically and kinetically favored radical cation intermediate **INT7**. The preference for this cation can be reasoned by the proximity to the nitrogen

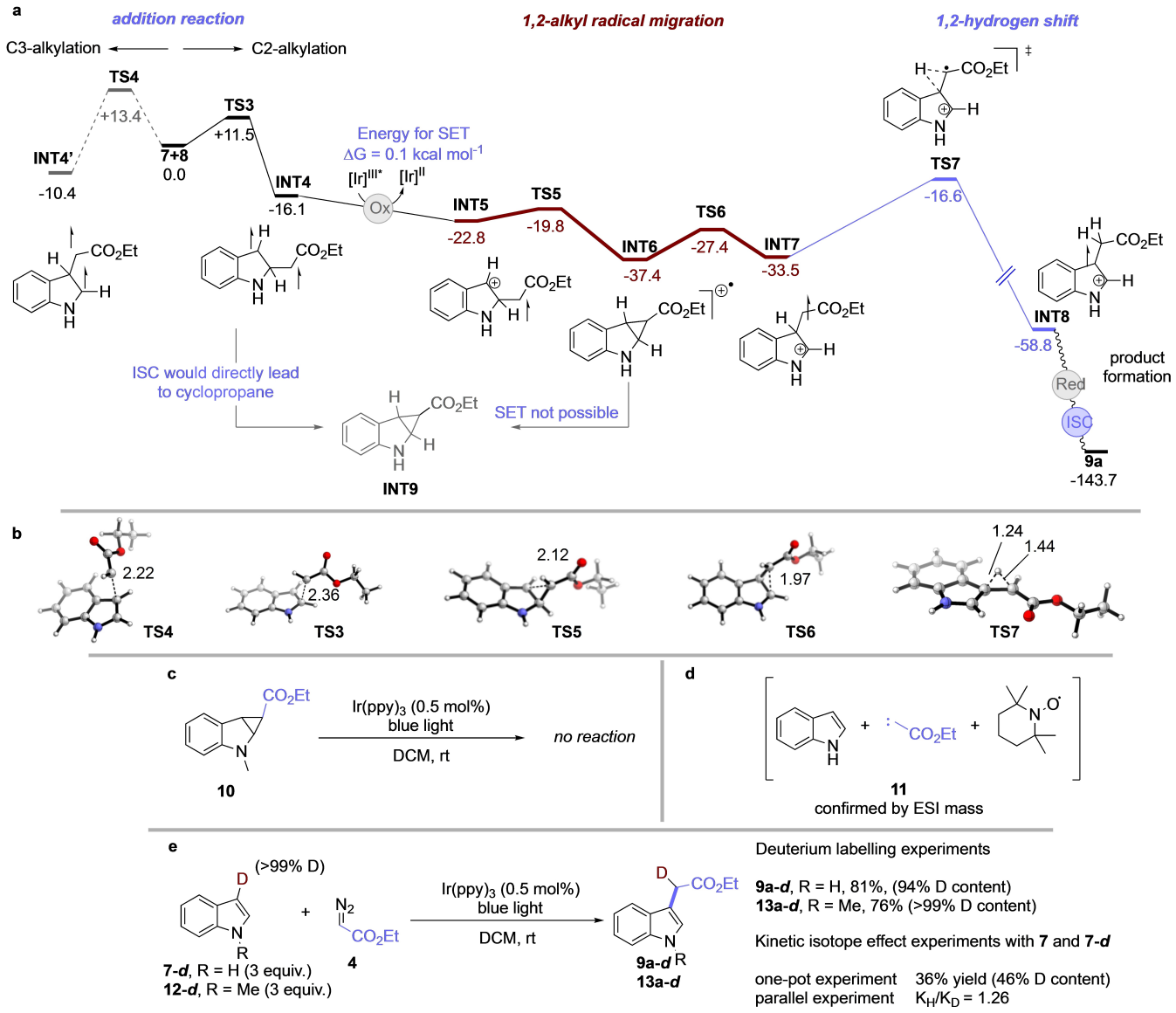

Scheme 4. Mechanism of the 1,2-alkyl radical migration. Calculations were performed at the (U)M06-2X-D3/def2-TZVPP // (U)B3LYP-D3BJ/def2-SVP/def2-TZVPP level of theory using SMD (DCM) solvent model. a. theoretical calculations on the reaction mechanism. b. 3D structures of key transition states. c. reaction of cyclopropyl indole. d. Observed adduct upon trapping of a reaction mixture with TEMPO after 2 h reaction time. e. deuterium labelling and kinetic isotope effect studies.

atom and stabilization by mesomeric effects. A subsequent intramolecular 1,2-hydrogen atom transfer occurs via transition state **TS7** with an activation free energy of 16.9 kcal/mol, which is sufficiently low to occur at room temperature and should result in the complete transfer of a deuterium label. Finally, reduction of radical cation intermediate **INT8** by the photoredox catalyst leads either to triplet intermediate that, upon intersystem crossing, gives the reaction product, or to open-shell or closed-shell singlet species that directly give the reaction product.

To probe the viability of this reaction mechanism, we considered alternative pathways. First, intersystem crossing of addition product **INT4** from triplet to singlet spin surface is not feasible and calculations further suggest the direct formation of a cyclopropane intermediate (see below, Figure S4). Second, we examined a potential single electron reduction of the cyclopropane radical cation **INT6** by the photoredox catalyst, however, this reduction is not feasible under the present reaction conditions (for details please see Figure S4).

We then embarked on the experimental validation of the above calculations. In an on/off experiment, we observed that light is required for the reaction to proceed (Figure S10). We further examined the reaction of cyclopropane **10** in the presence of the $Ir(ppy)_3$ photocatalyst, yet such cyclopropane is stable under the developed reaction conditions (Scheme 4c). Next, we aimed at trapping of intermediates with unpaired electrons. One-pot trapping experiments with TEMPO, DNP, or DMPO gave an almost complete inhibition of the reaction and

the adduct **11** of TEMPO with an intermediate carbene was observed by ESI-MS analysis (Scheme 4d). When adding the trapping reagent after 2 h reaction time, we observed the three-components-adduct consisting of indole, the carbene fragment of EDA and TEMPO or PBN. The exact structure of these adducts could not be identified (Scheme 4d, for details please see Supporting Information Figure S10 and S11). Similarly, EPR data is further suggestive of the intermediacy of complex radical species (Figure S19). In this context, we also examined a competition reaction of EDA using a 1 : 1 mixture of indole and *E*-β-methyl styrene or *Z*-β-methyl styrene, respectively. In this case, the reaction product of indole alkylation **9** was observed in significantly reduced yield and cyclopropanation occurred predominantly. Importantly, disregarding of the stereochemistry of the olefin used, a similar distribution of stereoisomers of the cyclopropane product was obtained, which is supportive of triplet carbene intermediates in the course of this photocatalytic reaction (See Supporting Information).[24]

We next examined the reaction of 3-deuterio indole **7-*d*** and the methylated analogue **12-*d***. In this case, the deuterium label was quantitatively sustained in the reaction product, which suggests that mechanisms involving a hypothetical intermolecular proton or hydrogen atom transfer or enalization do not contribute to product formation. Further analysis of the kinetic isotope effect from parallel and competition experiments showed no or only little influence of the deuterium label on the reaction rate for indole and deuterated indole (Scheme 4e).

In summary, the combined theoretical and experimental data provides evidence that C3-functionalization of indole heterocycles is possible via participation of triplet carbene intermediates. A mechanism involving C2-functionalization followed by [1,2]-alkyl radical and [1,2]-hydrogen atom migration can account for the observed reactivity.

Applications in synthesis

Finally, we turned towards the application of the developed method. A variety of core-substituted, unprotected indole derivatives, bearing either electron-donating or -withdrawing substituents, were well tolerated under this reaction conditions and the corresponding C3-functionalization products were obtained in high yield (Scheme 5). Substituents at the 2- and 4-position of indole, or free hydroxy groups did not have a significant influence on the reaction outcome. We next subjected different *N*-protected indole derivatives to the present reaction conditions. In all cases the corresponding C3-functionalization products were formed selectively in good to excellent yield - double bonds in the side chain remained untouched. Similarly, pyrrole derivatives proved compatible in this C–H functionalization reaction, which selectively occurred at the 2-position of pyrroles representing the classic nucleophilic position of pyrroles in alkylation reactions. Upon blocking the 2 and 5 position of pyrroles, the C3-functionalization product was obtained exclusively without any by-products arising from N–H functionalization. The limitations of the present method lie within the use of indazole or pyrrolopyridines, for which decomposition of the diazoalkane was observed.

In a next step, the influence of different alkyl diazoacetates was investigated, which reacted smoothly to give the desired products in good yield (Scheme 5). Here a broad range of different oxygen- or nitrogen-containing heterocycles, unsaturated bonds, naturally occurring alcohols, protected sugars or terpenes were found compatible and in all cases the respective C–H functionalization products were obtained with exclusive C3-selectivity and in good to high isolated yield.

To check the practical application of this method, we performed the reaction for indole **7** and *N*-methyl indole **12** on a 2 mmol scale (Scheme 6a). In both cases, the corresponding C3-alkylation products were isolated in 61% and 72% yield, respectively. Subsequent reduction with lithium aluminum hydride gave tryptophol **17a** and its *N*-methylated analogue **17b** in excellent yields. To further underline the importance of this method we showed that, *N*-methyl tryptophol **17b** can be converted to the carbazole derivative **19** in good yield via a borontrifluoride-promoted cascade reaction with propargylic alcohol **18**.[25] In another reaction, tryptophol **17a** was transformed to a 3-azidofuroindoline under copper-catalyzed conditions via a cascade azidation-cyclization reaction (Scheme 6b).[26]

Conclusion

A distinct photocatalytic 1,2-alkyl radical migration opens up pathways to the C3 functionalization of unprotected indole heterocycles. In a combined computational and experimental study, we show that the photocatalytic decomposition of diazoesters can lead either to a radical or triplet carbene intermediate depending on the solvent. While the radical intermediate engages in C2 functionalization, the triplet carbene allows for the C3 functionalization via initial C2 functionalization followed by a 1,2-alkyl radical shift and 1,2-hydrogen shift. This protocol was employed in a broad substrate scope (46 examples, up to 93% yield) and enables an efficient route towards the synthesis of tryptophol derivatives.

Experimental Section

General procedure for the C-H functionalization of indole: In an oven-dried reaction tube indole **7** (0.6 mmol, 3 equiv.), $Ir(ppy)_3$ (0.5 mol%) and one stirring bar were added. Then the tube was closed with septum and wrapped with parafilm. Reaction tube was evacuated and backfilled with argon for three times. Ethyl diazoacetate **4** (0.2 mmol, 1 equiv.) was dissolved in 1.0 mL dry, degassed DCM in a separate tube under argon atmosphere and the resulting solution was added to the reaction tube by syringe. Then the final reaction mixture was degassed for 30 seconds. Finally, the puncture hole in the septum was sealed with parafilm. The reaction mixture was irradiated with blue LED (2×Kessil PR160 L, 467 nm, 40 W) for 8 h at a distance of ~3 cm from the LED, temperature was maintained at room temperature with a cooling fan. After completion of the reaction, the product was purified by column chromatography on silica gel (*n*-Hexane:EtOAc).

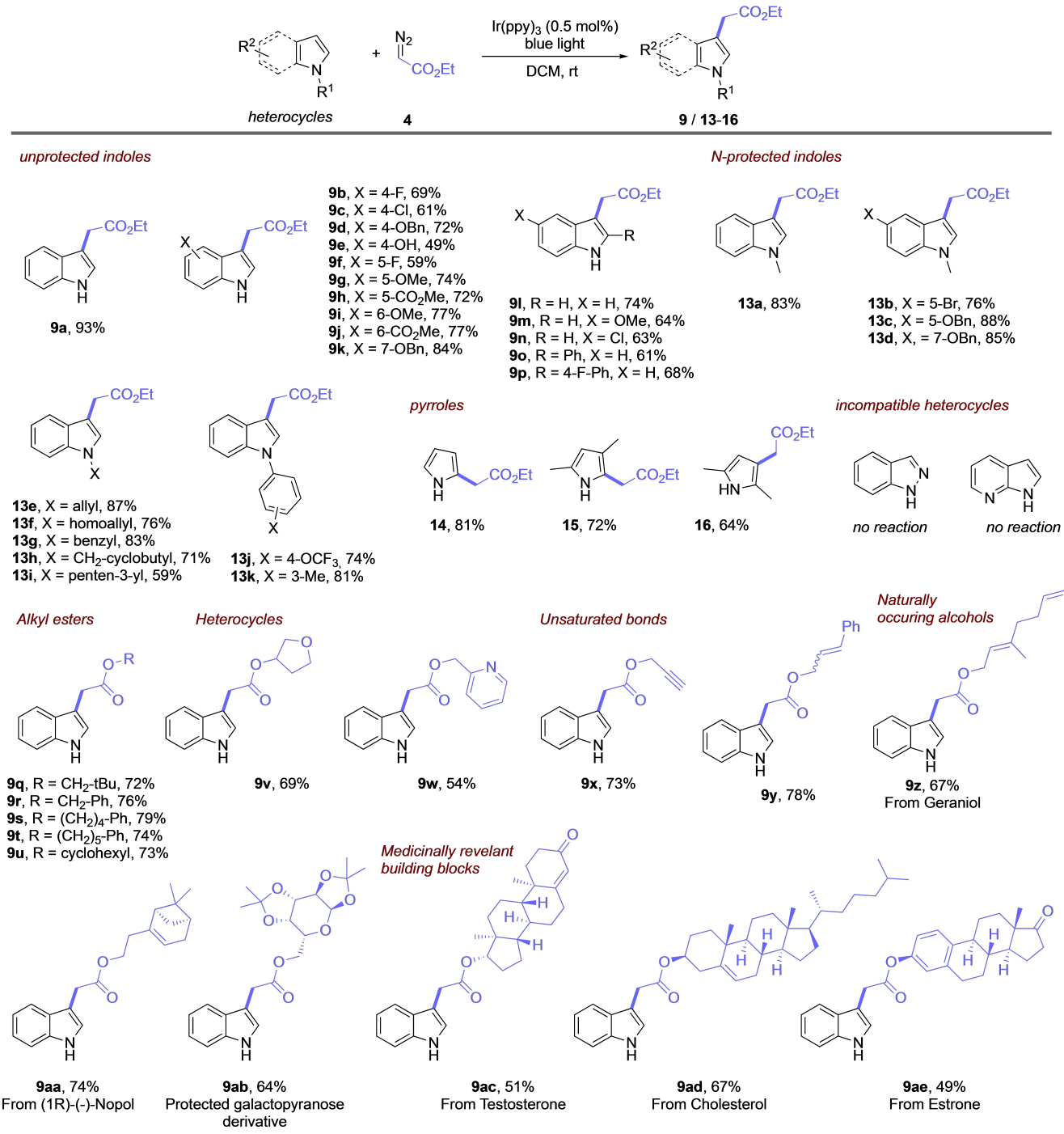

Scheme 5. Substrate scope of heterocycles and diazoacetates. Reaction condition: $Ir(ppy)_3$ (0.5 mol%), indole (0.6 mmol, 3 equiv.) and EDA (0.2 mmol, 1 equiv.) in 1 mL dry and degassed DCM under argon atmosphere were irradiated under 40-watt blue LED (467 nm) for 8 h.

Computational Details: All the calculations were performed with the Gaussian 16 program. Structure optimization was performed using the B3LYP functional[28] with Grimme's dispersion correction (denoted (U)B3LYP-D3),[29] and the def2-SVP basis set[30] for all H, C, N, O and the triple-ζ basis set def2-TZVPP for Ir.[29] Harmonic vibrational frequencies were calculated at the same level for all stationary points to confirm them as a local minima or transition structures. Key transition-state structures were confirmed to connect corresponding reactants and products by intrinsic reaction coordinate (IRC) calculations.[31] To improve the calculation accuracy, single point calculations were performed using the M06-2X functional[32] with Grimme's dispersion correction (denoted (U)M06-2X-D3), and the def2-TZVPP basis set[30] for all atoms. Furthermore, we have also considered the solvent effects in dichloromethane (ε = 8.93) or methanol (ε = 32.61) using the SMD solvation model,[33] for all structure optimizations and single-point energy calculations. The barriers of single electron transfer (SET) steps in this work were estimated using Marcus-Hush theory.[34] The CYL View software was employed to show the 3D structures of the studied species.[35]

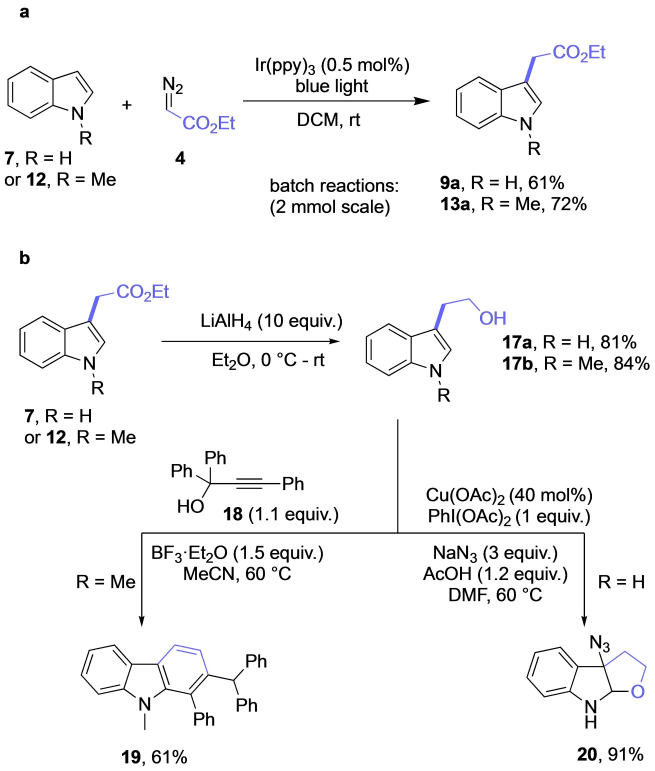

Scheme 6. Applications. a. Gram scale synthesis. b. Downstream functionalization.

Acknowledgements

RMK thanks the German Science Foundation for financial support. CE acknowledges the Fonds der Chemischen Industrie for a Kekulé scholarship. C.P. acknowledges the China Scholarship Council for financial support. The National Science Centre, Poland is acknowledged by DG, grant OPUS UMO-2019/35/B/ST4/03435. Open Access funding enabled and organized by Projekt DEAL.

Conflict of Interest

The authors declare no conflict of interest.

Data Availability Statement

The data that support the findings of this study are available in the supplementary material of this article.

Keywords: carbene · C–H functionalization · DFT calculations · photocatalysis · triplet

[1] F. Ehrlich, *Ber. Dtsch. Chem. Ges.* **1912**, *45*, 883–889.
[2] A. Vilela, *Fermentatio* **2019**, *5*, 46.
[3] A. Palmieri, M. Petrini, *Nat. Prod. Rep.* **2019**, *36*, 490–530.
[4] L. G. Humber, E. Ferdinandi, C. A. Demerson, S. Ahmed, U. Shah, D. Mobilio, J. Sabatucci, B. De Lange, F. Labbadia, P. Hughes, J. DeVirgilio, G. Neuman, T. T. Chau, B. M. Weichman, *J. Med. Chem.* **1988**, *31*, 1712–1719.
[5] A. Lippoldt, R. Bode, D. Birnbaum, *J. Basic Microbiol.* **1986**, *26*, 146–154.
[6] S. J. Garden, R. B. da Silva, A. C. Pinto, *Tetrahedron* **2002**, *58*, 8399–8412.
[7] K. J. Hock, A. Knorrscheidt, R. Hommelsheim, J. Ho, M. J. Weissenborn, R. M. Koenigs, *Angew. Chem. Int. Ed.* **2019**, *58*, 3630–3634; *Angew. Chem.* **2019**, *131*, 3669–3673.
[8] M. Delgado-Rebollo, A. Prieto, P. J. Pérez, *ChemCatChem* **2014**, *6*, 2047–2052.
[9] A. DeAngelis, V. W. Shurtleff, O. Dmitrenko, J. M. Fox, *J. Am. Chem. Soc.* **2011**, *133*, 1650–1653.
[10] X. Gao, B. Wu, W.-X. Huang, M.-W. Chen, Y.-G. Zhou, *Angew. Chem. Int. Ed.* **2015**, *54*, 11956–11960; *Angew. Chem.* **2015**, *127*, 12124–12128.
[11] D. A. Vargas, A. Tinoco, V. Tyagi, R. Fasan, *Angew. Chem. Int. Ed.* **2018**, *57*, 9911–9915; *Angew. Chem.* **2018**, *130*, 10059–10063.
[12] O. F. Brandenberg, K. Chen, F. H. Arnold, *J. Am. Chem. Soc.* **2019**, *141*, 8989–8995.
[13] Z. Yang, M. Möller, R. M. Koenigs, *Angew. Chem. Int. Ed.* **2020**, *59*, 5572–5576; *Angew. Chem.* **2020**, *132*, 5620–5624.
[14] Ł. W. Ciszewski, J. Durka, D. Gryko, *Org. Lett.* **2019**, *21*, 7028–7032.
[15] C. Empel, C. Pei, C. R. M. Koenigs, *Chem. Commun.* **2022**, *58*, 2788–2798.
[16] a) Ł. W. Ciszewski, K. Rybicka-Jasińska, D. Gryko, *Org. Biomol. Chem.* **2019**, *17*, 432–448; b) Z. Yang, M. L. Stivanin, I. D. Jurberg, R. M. Koenigs, *Chem. Soc. Rev.* **2020**, *49*, 6833–6847; c) C. Empel, C. Pei, R. M. Koenigs, *Chem. Commun.* **2022**, *58*, 2788–2798; d) Y. Xie, J. Xuan, *Chin. J. Org. Chem.* **2022**, *42*, 4247–4256; e) J. Durka, J. Turkowska, D. Gryko, *ACS Sustainable Chem. Eng.* **2021**, *9*, 8895–8918.
[17] H. M. L. Davies, J. R. Manning, *Nature* **2008**, *451*, 417–424.
[18] C. Empel, S. Jana, R. M. Koenigs, *Molecules* **2020**, *25*, 880.
[19] X. Huang, R. D. Webster, K. Harms, E. Meggers, *J. Am. Chem. Soc.* **2016**, *138*, 12636–12642.
[20] Y.-L. Su, G.-X. Liu, J.-W. Liu, L. Tram, H. Qiu, M. P. Doyle, *J. Am. Chem. Soc.* **2020**, *142*, 13846–13855.
[21] a) F. Li, C. Pei, R. M. Koenigs, *Angew. Chem. Int. Ed.* **2022**, *61*, e202111892; b) F. Li, S. Zhu, R. M. Koenigs, *Chem. Commun.* **2022**, *58*, 7526–7529; c) S. Zhu, F. Li, C. Empel, S. Jana, C. Pei, R. M. Koenigs, *Adv. Synth. Catal.* **2022**, *364*, 3149–3154.
[22] Y. Liu, K. Zhu, P. Li, *Org. Lett.* **2022**, *24*, 6834–6838.
[23] K. Rybicka-Jasińska, W. Shan, K. Zawada, K. M. Kadish, D. Gryko *J. Am. Chem. Soc.* **2016**, *138*, 15451–15458.
[24] T. Langletz, C. Empel, S. Jana, R. M. Koenigs, *Tetrahedron Chem* **2022**, *3*, 100024.
[25] C. K. Prier, D. A. Rankic, D. W. C. MacMillan, *Chem. Rev.* **2013**, *113*, 5322–5363.
[26] K. Huang, G. Sheng, P. Lu, Y. Wang, *Org. Lett.* **2017**, *19*, 4114–4117.
[27] P. Zhang, W. Sun, G. Li, L. Hong, R. Wang, *Chem. Commun.* **2015**, *51*, 12293–12296.
[28] a) A. D. Becke, *J. Chem. Phys.* **1993**, *98*, 5648–5652; b) C. Lee, W. Yang, R. G. Parr, *Phys. Rev. B: Condens. Matter Mater. Phys.* **1988**, *37*, 785–789.
[29] F. Weigend, R. Ahlrichs, *Phys. Chem. Chem. Phys.* **2005**, *7*, 3297–3305.
[30] S. Grimme, J. Antony, S. Ehrlich, H. Krieg, *J. Chem. Phys.* **2010**, *132*, 154104.
[31] a) K. Fukui, *J. Phys. Chem.* **1970**, *74*, 4161–4163; b) K. Fukui, *Acc. Chem. Res.* **1981**, *14*, 363–368.
[32] Y. Zhao, D. G. Truhlar, *Theor. Chem. Acc.* **2008**, *120*, 215–41.
[33] A. V. Marenich, C. J. Cramer, D. G. Truhlar, *J. Phys. Chem. B* **2009**, *113*, 6378–6396.
[34] R. A. Marcus, *J. Chem. Phys.* **1956**, *24*, 966–978.
[35] C. Y. Legault, **2020**, CYLview, 1.0b, Universitéde Sherbrooke. http://www.cylview.org.

Manuscript received: January 21, 2023
Accepted manuscript online: March 6, 2023
Version of record online: April 13, 2023